RESEARCH PAPER

Epigenetics 8:8, 849–863; August 2013; © 2013 Landes Bioscience

DNA methylation and nucleosome occupancy regulate the cancer germline antigen gene *MAGEA11*

Smitha R James,[1,†,‡] Carlos D Cedeno,[1,†] Ashok Sharma,[2] Wa Zhang,[1,2] James L Mohler,[3] Kunle Odunsi,[4] Elizabeth M Wilson[5] and Adam R Karpf[1,2,*]

[1]Department of Pharmacology and Therapeutics; Roswell Park Cancer Institute; Buffalo, NY USA; [2]Eppley Institute for Research in Cancer; University of Nebraska Medical Center; Omaha, NE USA; [3]Department of Urology; Roswell Park Cancer Institute; Buffalo, NY USA; [4]Departments of Immunology, Gynecologic Oncology, and Center for Immunotherapy; Roswell Park Cancer Institute; Buffalo, NY USA; [5]Department of Pediatrics, Biochemistry and Biophysics; Lineberger Comprehensive Cancer Center; University of North Carolina; Chapel Hill, NC USA

[†]These authors contributed equally to this work.

[‡]Current affiliation: Center of Excellence in Bioinformatics and Life Sciences; University at Buffalo; Buffalo, NY USA

Keywords: DNA methylation, epigenetics, nucleosome occupancy, cancer germline genes, cancer testis genes, MAGEA11

Abbreviations: AS, androgen-sensitive prostate cancer; BP, benign prostatic hyperplasia; CG, cancer-germline; ChIP, chromatin immunoprecipitation; CR, castration-recurrent prostate cancer; DAC, 5-aza-2'-deoxycytidine; DKO cells, HCT116 *DNMT1*$^{-/-}$, *3b*$^{-/-}$ double knockout cells; DNMT, cytosine DNA methyltransferase; EOC, epithelial ovarian cancer; HDAC, histone deacetylase; MAGEA11, melanoma antigen a11; MAPit, methyltransferase accessibility protocol for individual templates; MitA, mithromycin A; NO, normal ovary; RT-qPCR, reverse transcriptase quantitative PCR; TIC, transcriptional initiation complex; TSA, Trichostatin A; TSS, transcriptional start site

MAGEA11 is a cancer germline (CG) antigen and androgen receptor co-activator. Its expression in cancers other than prostate, and its mechanism of activation, has not been reported. In silico analyses reveal that *MAGEA11* is frequently expressed in human cancers, is increased during tumor progression, and correlates with poor prognosis and survival. In prostate and epithelial ovarian cancers (EOC), *MAGEA11* expression was associated with promoter and global DNA hypomethylation, and with activation of other CG genes. Pharmacological or genetic inhibition of DNA methyltransferases (DNMTs) and/or histone deacetylases (HDACs) activated *MAGEA11* in a cell line specific manner. *MAGEA11* promoter activity was directly repressed by DNA methylation, and partially depended on Sp1, as pharmacological or genetic targeting of Sp1 reduced *MAGEA11* promoter activity and endogenous gene expression. Importantly, DNA methylation regulated nucleosome occupancy specifically at the -1 positioned nucleosome of *MAGEA11*. Methylation of a single Ets site near the transcriptional start site (TSS) correlated with -1 nucleosome occupancy and, by itself, strongly repressed *MAGEA11* promoter activity. Thus, DNA methylation regulates nucleosome occupancy at *MAGEA11*, and this appears to function cooperatively with sequence-specific transcription factors to regulate gene expression. *MAGEA11* regulation is highly instructive for understanding mechanisms regulating CG antigen genes in human cancer.

Introduction

Cancer testis or germline (CG) antigen genes are expressed in germ cells and human tumors and encode immunogenic tumor antigens.[1,2] Vaccines targeting CG antigens are undergoing clinical testing in a variety of human malignancies that include melanoma, lung, and ovarian cancers.[2] In addition to their significance as immunotherapy targets, CG gene products may contribute to oncogenesis. In particular, the MAGE gene family contains a MAGE homology domain (MHD), which in some instances can serve as a binding module for the RING family of ubiquitin E3 ligases to promote degradation of the tumor suppressor protein p53.[3] MAGEA11 facilitates co-activator recruitment to the androgen receptor (AR) in the absence and presence of ligand, leading to activation of AR target genes in prostate cancer.[4] Other CG genes make distinct contributions to oncogenesis.[5-9] These studies suggest that CG antigen proteins have potential as therapeutic targets, beyond their current role in cancer immunotherapy.

We previously reported that the *MAGEA11* promoter CpG island is hypermethylated in benign prostatic intraepithelial

*Correspondence to: Adam R Karpf; Email: adam.karpf@unmc.edu
Submitted: 05/26/13; Revised: 06/18/13; Accepted: 06/21/13
http://dx.doi.org/10.4161/epi.25500

neoplasia, but can become hypomethylated in prostate cancer, particularly in castration-recurrent disease, and that this occurs in conjunction with gene activation.[10] MAGEA11 appears to make a specific contribution to prostate cancer via its myriad of effects on AR signaling.[4] However, two fundamental questions remain. First, is MAGEA11 activation a specifically selected event, or is it associated with activation of other CG genes, as a result of a global epigenetic alteration, e.g., global DNA hypomethylation?[11] Second, is MAGEA11 activated in human cancers other than prostate and, if so, does this result from epigenetic alterations?

DNA methylation is intertwined with other epigenetic mechanisms that include histone acetylation, histone methylation, and nucleosome occupancy.[12] Studies aimed to discern the relationship among these interdependent mechanisms at genes epigenetically activated in cancer, which include CG antigens, are limited. Recent work has explored the role of DNA methylation and histone modifications in CG antigen gene regulation,[13-16] but information is lacking about the role of nucleosome occupancy in CG antigen gene regulation, or how this relates to other epigenetic marks. Also, epigenetic remodeling alone appears insufficient for CG gene activation, which additionally requires the action of sequence-specific transcription factors.[1,17] How diverse epigenetic mechanisms and transcription factors are integrated to promote CG gene expression in cancer is unresolved.

An in silico analysis of *MAGEA11* gene expression was conducted in human cancer to begin to address these questions. Cell lines and primary tissues from prostate and epithelial ovarian cancers (EOC) were analyzed to determine the relationship among *MAGEA11* expression, promoter DNA hypomethylation, and global DNA hypomethylation. Genetic and pharmacological approaches were applied to cancer cell lines to determine the relationship among DNA methylation, histone acetylation, and *MAGEA11* gene expression. Promoter luciferase approaches addressed the impact of DNA methylation on *MAGEA11* promoter activity, and investigated the role of Sp1 in *MAGEA11* gene regulation. The novel Methyltransferase Accessibility Protocol for individual templates (MAPit) sequencing method was used to assess the role of nucleosome occupancy in *MAGEA11* gene regulation, and to determine how it is influenced by DNA methylation.

Results

***MAGEA11* expression is elevated in multiple human cancers and is coordinately expressed with other CG antigen genes.** We reported previously that *MAGEA11* expression increases in castration-recurrent prostate cancer in a relatively small number of clinical specimens.[10] To expand this analysis, we used *Oncomine* to analyze publically available microarray data sets for *MAGEA11* expression in prostate cancer and to determine the possible relationship to clinicopathology. This analysis confirmed *MAGEA11* expression in prostate cancer, and revealed significantly increased expression with increased Gleason grade (**Fig. 1A**), progression to metastasis (**Fig. 1B**), and in patients with early disease recurrence (**Fig. 1C**). To determine whether *MAGEA11* expression in prostate cancer is associated with activation of other CG antigen genes, we measured *MAGEA11* and three representative CG genes, *MAGEA1*, *NY-ESO1* and *XAGE1,* in benign or malignant human prostate cells. Each of the CG genes was not significantly expressed in benign prostate cell lines, but was heterogeneously expressed in prostate cancer cell lines (**Fig. 1D**). *MAGEA11* was low to moderately expressed in benign prostate and most cancer cell lines, and elevated in LAPC-4 cells (**Fig. 2A**). LAPC-4 also displayed the highest expression of other CG genes (**Fig. 1D**). To further assess the correlation between *MAGEA11* and other CG gene expression, we analyzed primary prostate tissue samples, which included benign prostatic hyperplasia (BP), androgen-stimulated prostate cancer (AS), and castration-recurrent prostate cancer (CR). *MAGEA11* was highly expressed in a CR sample (CR1), that also was the only sample with significant expression of other CG genes (**Fig. 1E**). The data suggest that *MAGEA11* is expressed concordantly with other CG genes in prostate cancer. Next, *Oncomine* was used to determine whether *MAGEA11* is expressed in human cancers other than prostate. We found that *MAGEA11* expression is elevated in a number of different human cancers, including esophageal and kidney (renal cell) tumors (**Fig. S1A and C**). *MAGEA11* was expressed in 20–40% of these lesions, and its expression correlated with that of other *MAGEA* genes (data not shown). Furthermore, in both tumor types, *MAGEA11* expression was associated with poor prognosis, similar to prostate cancer (**Fig. S1B and D**). We also analyzed *MAGEA11* expression in human EOC, which has proven a useful disease model to study CG antigen gene regulation.[18-20] *Oncomine* analysis of the Cancer Genome Atlas (TCGA) high-grade serous ovarian cancer data revealed significant elevation of *MAGEA11* expression in EOC as compared with normal ovary (**Fig. 2A**). *MAGEA11* was expressed in ~20% of EOC lesions in the TCGA (i.e., above the *Oncomine* median expression value and significantly elevated compared with normal ovary). Spurred by these data, we directly examined *MAGEA11* expression in a set of primary EOC tissues. We used *Affymetrix HG 1.0 ST* microarrays to analyze the expression of *MAGEA11* and other CG antigens in three NO and 40 EOC tissues described earlier.[19] In agreement with the TCGA data, we observed significant elevation of *MAGEA11* in EOC compared with NO (**Fig. 2B**). The TCGA data was explored further to determine whether *MAGEA11* expression correlates with other CG genes. Genes with the highest correlation to *MAGEA11* were known CG antigen genes, including other *MAGEA* family members (**Fig. 2C**). In agreement with the TCGA, *MAGEA11* expression correlated with other CG antigen genes in our EOC sample set (**Fig. 2D**).

***MAGEA11* expression is associated with DNA hypomethylation at its TSS.** In our previous analysis of prostate cancer cell lines, we observed DNA methylation proximal to the predicted *MAGEA11* TSS, rather than at the 5' end of the promoter CpG island.[10] Bisulfite clonal sequencing was performed in the normal PWR-1E prostate epithelial cell line, which has low *MAGEA11* expression, to determine whether proximal promoter methylation is critical for *MAGE-A11* expression (**Fig. 3A**). PWR-1E cells displayed partial DNA methylation throughout most of the

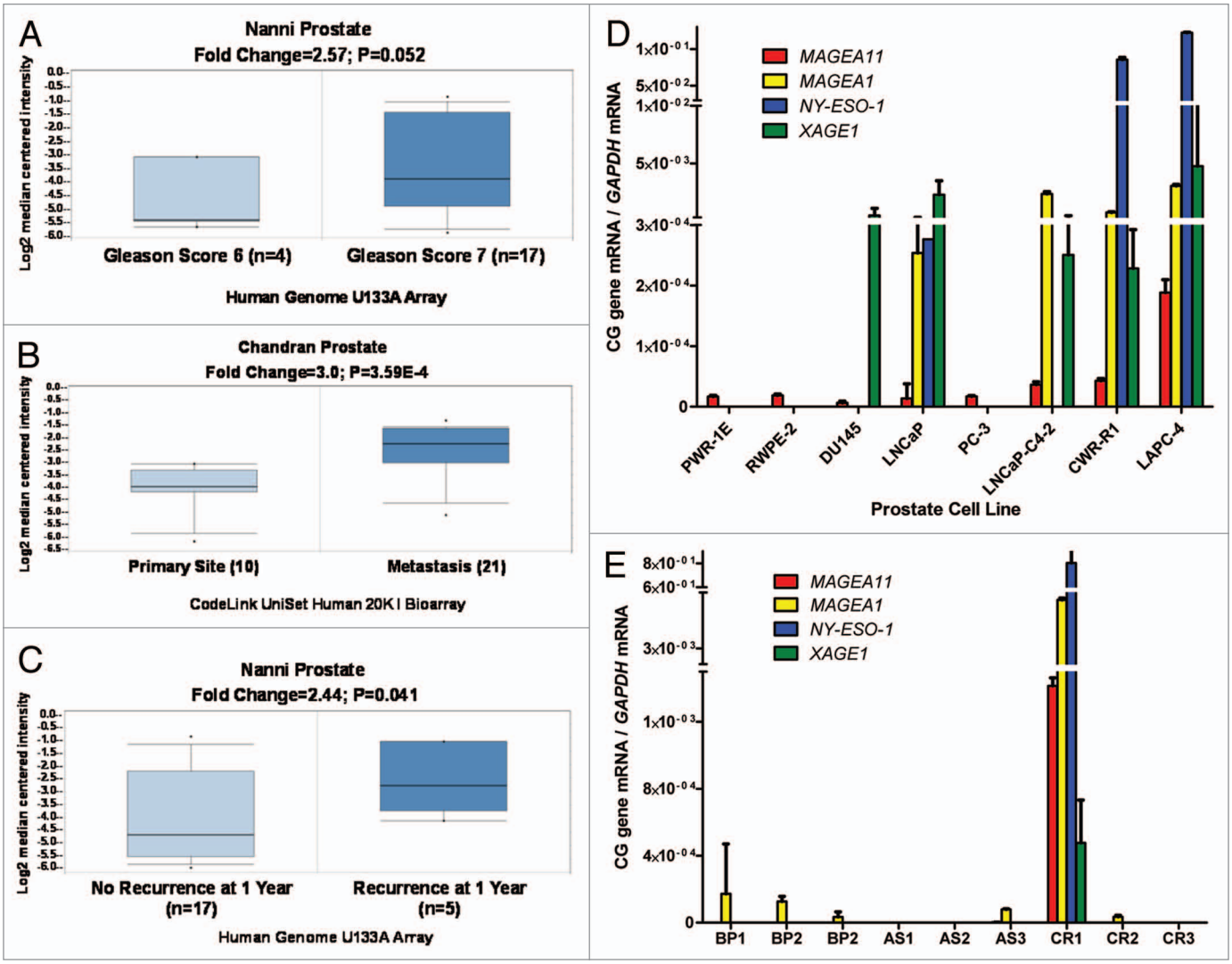

Figure 1. *MAGEA11* expression in human prostate cancer. (**A–C**) *Oncomine* analysis of *MAGEA11* expression. Fold change, P-value, and microarray platform is indicated, and the title shows the first author of the referenced studies.[61,62] Data are presented as a box and whiskers plot, with the box indicating the 25th to 75th percentiles, whiskers indicating the 10th and 90th percentiles, top and bottom points indicating the range, and center line indicating the median. (**A**) *MAGEA11* expression as a function of prostate cancer Gleason grade. (**B**) *MAGEA11* expression in primary and metastatic prostate cancer. (**C**) *MAGEA11* expression as a function of prostate cancer recurrence at one year. (**D**) Expression of *MAGEA11* and three representative CG antigen genes, *MAGEA1*, *NY-ESO-1* and *XAGE1* in prostate cell lines was measured using RT-qPCR. PWR-1E and RWPE-2 are cell lines derived from benign prostate epithelium, while the other cell lines were derived from prostate cancers. (**E**) Gene expression was measured as described in (**D**), using primary tissues derived from benign prostatic hyperplasia (BP), androgen-stimulated prostate cancer (AS), and castration-recurrent prostate cancer (CR). Absence of a bar indicates that no expression was detected.

5' CpG island, but the CpGs located adjacent to the predicted TSS were hypermethylated. Previously obtained methylation data for prostate cancer cell lines are shown for comparison[10] (**Fig. 3A**, TSS adjacent CpGs in red boxes), and *MAGEA11* expression and methylation in the four prostate cell lines analyzed are summarized in **Figure 3B**. *MAGEA11* was expressed at the highest level in LAPC-4 cells, the only cell type in which the TSS region is hypomethylated. RLM-RACE was used to map the TSS of *MAGEA11* in LAPC-4 cells, to confirm the relevance of our findings. The data confirmed that the TSS is located adjacent to the CpG sites showing differential methylation in the prostate cell lines (**Fig. 3A**, TSS indicated with right broken arrows). In addition to prostate cancer, we investigated DNA methylation relative to *MAGEA11* gene regulation in EOC. Initially, bisulfite clonal sequencing was performed on NO and EOC samples. The *MAGEA11* 5' CpG island and TSS region were moderately to highly methylated in both NO and EOC samples that had low levels of *MAGEA11* expression, but were hypomethylated in an EOC sample (EOC38) expressing high levels of *MAGEA11* (**Fig. 3C**). We developed a bisulfite pyrosequencing assay for *MAGEA11* TSS methylation, to enable analysis of a larger number of biological samples and statistical testing of this association. Pyrosequencing established a significant indirect association between *MAGEA11* expression and TSS methylation in EOC (**Fig. 3D**).

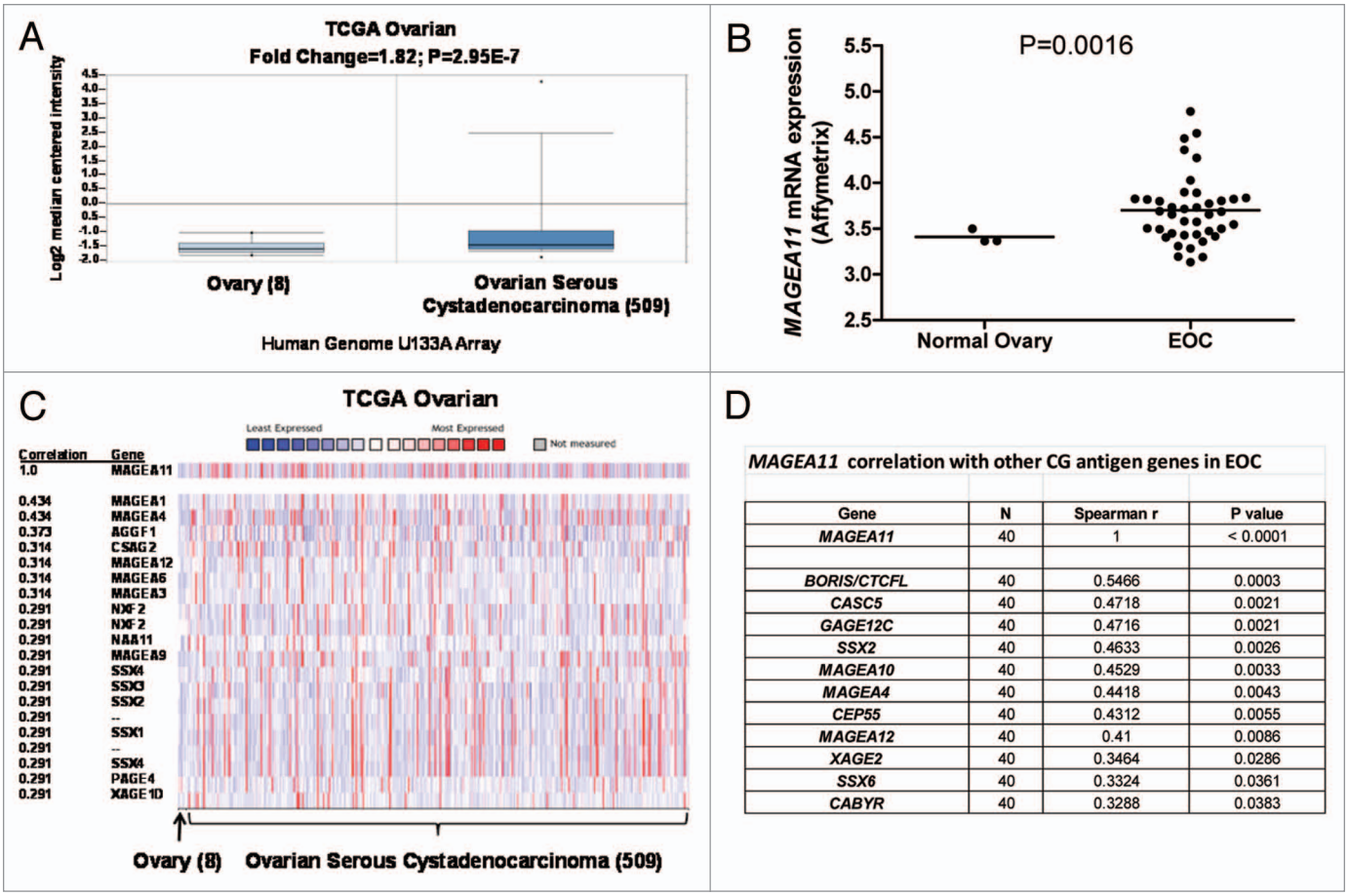

***MAGEA11* correlation with other CG antigen genes in EOC**

Gene	N	Spearman r	P value
MAGEA11	40	1	< 0.0001
BORIS/CTCFL	40	0.5466	0.0003
CASC5	40	0.4718	0.0021
GAGE12C	40	0.4716	0.0021
SSX2	40	0.4633	0.0026
MAGEA10	40	0.4529	0.0033
MAGEA4	40	0.4418	0.0043
CEP55	40	0.4312	0.0055
MAGEA12	40	0.41	0.0086
XAGE2	40	0.3464	0.0286
SSX6	40	0.3324	0.0361
CABYR	40	0.3288	0.0383

Figure 2. *MAGEA11* expression in epithelial ovarian cancer (EOC). (**A**) *Oncomine* analysis of *MAGEA11* mRNA expression in TCGA data.[63] Fold change, *P* value, and microarray platform is indicated. Data presentation is as described in **Figure 1**. (**B**) *Oncomine* analysis of the genes most closely correlated with *MAGEA11* in TCGA data. (**C**) *MAGEA11* mRNA expression was determined in three normal ovary samples and 40 EOC samples using Affymetrix HG 1.0ST microarrays. Two-tailed t-test results are shown. (**D**) Expression of *MAGEA11* and other CG antigen genes was determined by Affymetrix microarray, as described in (**C**). Spearman test r values and *P* values for correlation with *MAGEA11* are shown.

***MAGEA11* expression and hypomethylation is associated with global DNA hypomethylation.** We used *LINE1* methylation as a biomarker for global DNA methylation status to examine whether global DNA hypomethylation is related to *MAGEA11* activation in cancer.[19,20] *LINE1* pyrosequencing is a cost effective assay and readout for overall global methylation in cancer, as there is a direct correlation between *LINE1* and 5mdC in cancer tissues.[20] In prostate cell lines, an inverse correlation between *MAGEA11* expression and *LINE1* methylation was observed, but did not reach statistical significance (**Fig. 4A**; Spearman r = −0.455, p = 0.27). In clinical prostate tissues, *LINE1* was hypomethylated to the greatest extent in the CR tumor that expressed *MAGEA11* (**Fig. 4B**). We analyzed two groups of EOC lesions characterized by distinct *LINE1* methylation (i.e., hypomethylated and hypermethylated), and NO samples as controls, to more rigorously test this association (**Fig. 4C**). While *MAGEA11* expression was higher in both EOC sample groups compared with NO, its expression was highly elevated in hypomethylated vs. hypermethylated EOC (**Fig. 4C**). Moreover, there was a significant inverse correlation between *MAGEA11* expression and *LINE1* methylation in all EOC samples (**Fig. 4D**). The indirect association between *MAGEA11* expression and *LINE1* methylation suggested that *MAGEA11* methylation and *LINE1* methylation are associated. Consistent with this hypothesis, there was a significant association between *MAGEA11* TSS methylation and *LINE1* methylation in prostate cancer and EOC (**Fig. 4E and F**).

To further investigate the relationship between promoter and global DNA methylation and *MAGEA11* expression, we used a human colorectal cancer somatic cell genetic knockout system in which the cytosine DNA methyltransferase enzymes DNMT1 and DNMT3b have been targeted alone or in combination.[21] *MAGEA11* expression was undetectable in wild-type HCT116 cells, increased in single DNMT1 or DNMT3b knockout HCT116 cells, and was highest double knockout DNMT1/3b HCT116 cells (DKO) (**Fig. S2A**; note that expression was plotted on a log scale). In agreement with the expression results, the *MAGEA11* promoter was hypermethylated in wild-type HCT116 cells with progressively greater hypomethylation in DNMT3b$^{-/-}$, DNMT1$^{-/-}$, and DKO cells, respectively (**Fig. S2B**). These results support the idea that TSS hypomethylation is required for high *MAGEA11* expression, since only HCT116 DKO cells showed robust hypomethylation at the

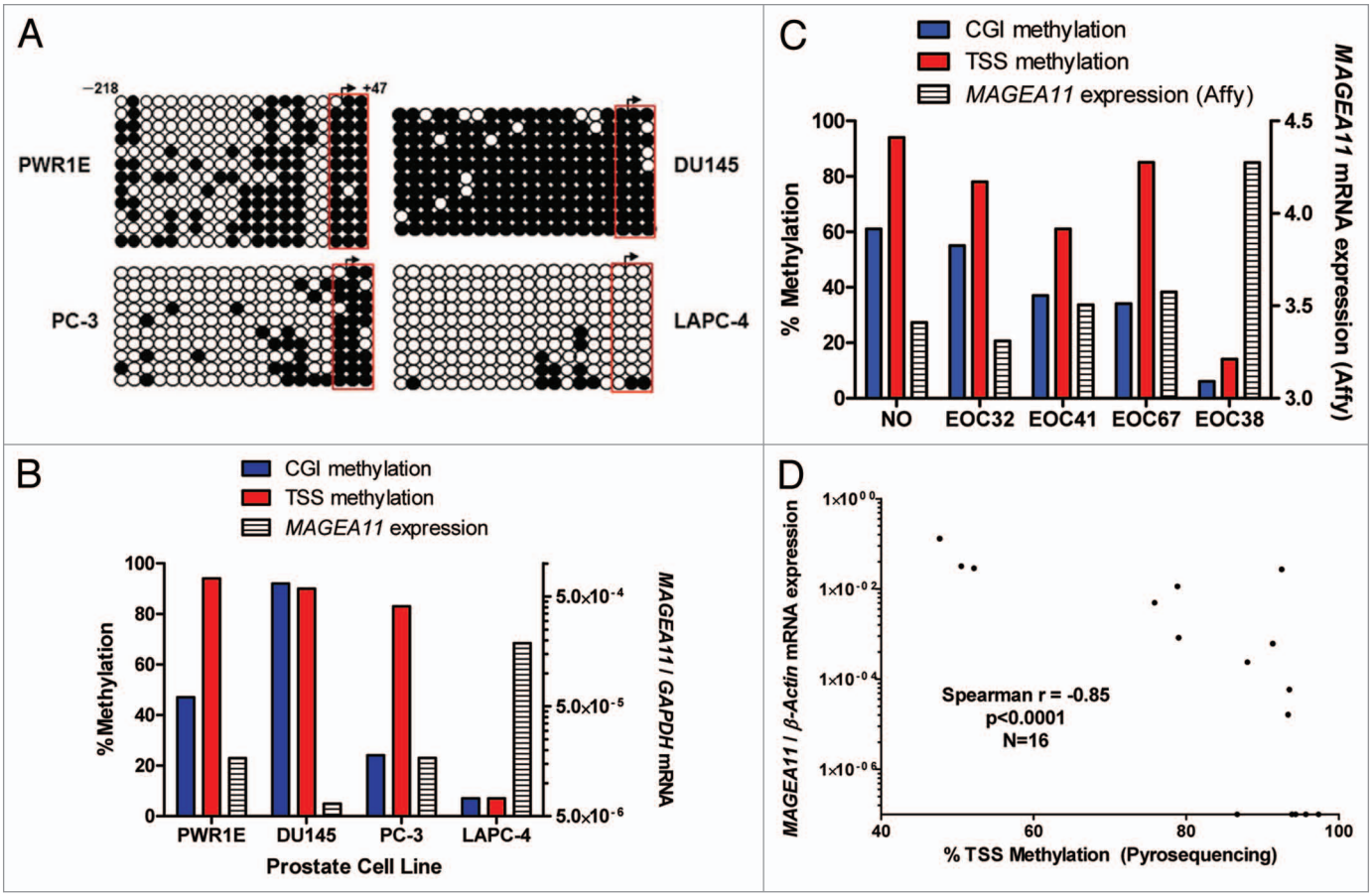

Figure 3. *MAGEA11* promoter methylation and expression in prostate cancer and EOC. (**A**) Sodium bisulfite clonal sequencing of the *MAGEA11* promoter region was performed on the indicated cell lines. The transcriptional start site (TSS), as determined by RLM-RACE, is indicated by the right broken arrow, and the coordinates of the analyzed region are shown in the upper left panel. Filled and open circles indicate methylated and unmethylated CpG sites, respectively, and each row represents one sequenced allele. The red box indicates three TSS-adjacent CpG sites. (**B**) Summary of *MAGEA11* bisulfite sequencing and mRNA expression data in prostate cell lines. Methylation percentages for the entire *MAGEA11* 5' CpG island (CGI) or for the three TSS-resident CpGs were calculated from (**A**), and *MAGEA11* expression was determined by RT-qPCR. (**C**) *MAGEA11* promoter methylation and mRNA expression in one normal ovary (NO) and four EOC samples were determined using bisulfite clonal sequencing (>10 alleles), and *Affymetrix* microarray, respectively. (**D**) *MAGEA11* mRNA expression indirectly correlates with *MAGEA11* TSS methylation in EOC. *MAGEA11* expression and methylation of three TSS-resident CpG sites in 16 EOC samples was determined by RT-qPCR and bisulfite pyrosequencing, respectively. Five samples that did not express measurable *MAGEA11* are plotted on the x-axis. Spearman test results are shown.

MAGEA11 TSS. The effect of DNMT loss on *MAGEA11* promoter methylation paralleled the effect on global DNA methylation in these cell lines,[14,21,22] which provides additional evidence for a link between global DNA hypomethylation and *MAGEA11* expression.

DNMT and histone deacetylase (HDAC) inhibitors induce *MAGEA11* expression in a cell type specific manner. In addition to DNA methylation, histone modification can play an important role in CG gene regulation.[14-16,23] A pharmacological approach was used in prostate cell lines to investigate the relative roles of DNA methylation and histone deacetylation on *MAGEA11* repression. Prostate cell lines were treated with the pan-DNMT inhibitor decitabine (DAC) and the pan-class I/II HDAC inhibitor Trichostatin A (TSA),[24,25] individually or in combination. Decitabine treatment was confirmed to reduce *MAGEA11* promoter DNA methylation levels (data not shown). In DU145 and PC-3 prostate cancer cells in which the *MAGEA11* TSS region is hypermethylated, *MAGEA11* was induced by decitabine but not by TSA, with the highest level of induction following combination treatment (**Fig. 5A and B**). These findings suggest that DNA methylation plays a primary role in *MAGEA11* gene repression, and histone deacetylation plays an accessory role, in cells with TSS-hypermethylated *MAGEA11*. In LAPC-4 cells, in which the *MAGEA11* TSS is hypomethylated, TSA caused substantial induction of *MAGEA11* while decitabine did not, although the combination treatment still showed the greatest effect (**Fig. 5C**). These findings suggest that HDACs can still repress *MAGEA11*, when TSS DNA methylation levels are lower. In agreement, ChIP analysis showed that TSA treatment increased histone acetylation at lysine 9 (H3K9-Ac) at the *MAGEA11* promoter in LAPC-4 cells (**Fig. S3A**). In contrast to DU145 and PC-3 cells, TSA treatment did not influence *MAGEA11* expression in benign PWR-1E prostate cells (**Fig. 5D**). This is suggestive of cancer-specific alterations in HDACs, as has been reported.[26]

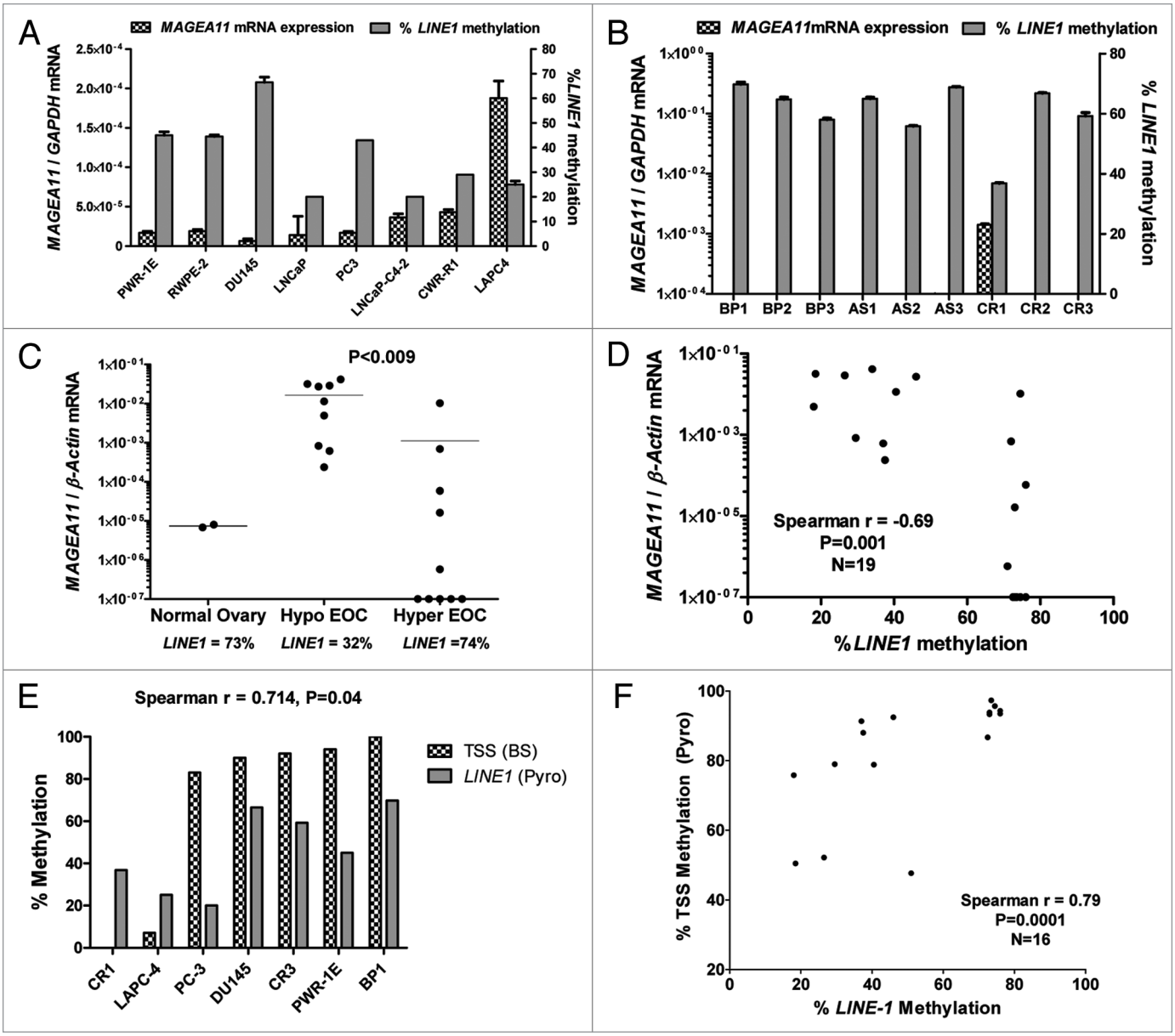

Figure 4. *MAGEA11* expression and methylation and global DNA methylation. (**A**) *MAGEA11* expression and *LINE1* methylation in human prostate cell lines. *MAGEA11* expression was determined by RT-qPCR and *LINE1* methylation was determined by pyrosequencing. PWR-1E and RWPE-2 are derived from normal prostate epithelium, while other cell lines are derived from prostate cancer. Spearman test showed an inverse association between *MAGEA11* expression and *LINE1* methylation, which did not reach statistical significance (R = −0.455, p = 0.267). (**B**) *MAGEA11* expression and *LINE1* methylation in primary prostate tissues. Measurements were determined as described in (**A**). (**C**) *MAGEA11* expression and *LINE1* methylation in normal ovary and EOC with divergent *LINE1* methylation. *MAGEA11* expression and *LINE1* methylation were determined as described in (**A**). *MAGEA11* expression is plotted on a log axis and note that five samples in the hypermethylated EOC group did not express measurable *MAGEA11*. The mean *LINE1* methylation level in three sample groups is shown below the x-axis. Two-tailed t-test results are shown. (**D**) *MAGEA11* expression and *LINE1* methylation are indirectly associated in EOC. *MAGEA11* expression was plotted vs. *LINE1* methylation in EOC samples from both EOC groups shown in (**C**). Spearman test results are shown. (**E**) *MAGEA11* TSS methylation and *LINE1* methylation are directly associated in prostate cancer. Methylation was determined using bisulfite sequencing (*MAGEA11*) and pyrosequencing (*LINE-1*). Spearman test results are shown. (**F**) *MAGEA11* TSS methylation and *LINE1* methylation are directly associated in EOC. Methylation was determined using pyrosequencing. Spearman test results are shown.

***MAGEA11* is directly repressed by DNA methylation, and activated by Sp1.** A luciferase reporter gene assay was used to determine the impact of DNA methylation on *MAGEA11* promoter activity in prostate cancer cells. Four constructs, C1 through C4, were prepared that terminate 55 bp downstream of the *MAGEA11* TSS and span different lengths upstream (**Fig. 6A**). Each construct was active in prostate cell lines, in the order, C3 > C2 > C1 > C4, in all 3 cell lines (**Fig. 6B**). Notably, C3, which contains a cluster of 10 CpG sites embedded within 10 consensus Sp1 binding sites, had the highest activity, while C4, which was identical to C3 but did not contain the Sp1 region, had the lowest activity (**Fig. 6A–C**). This suggested

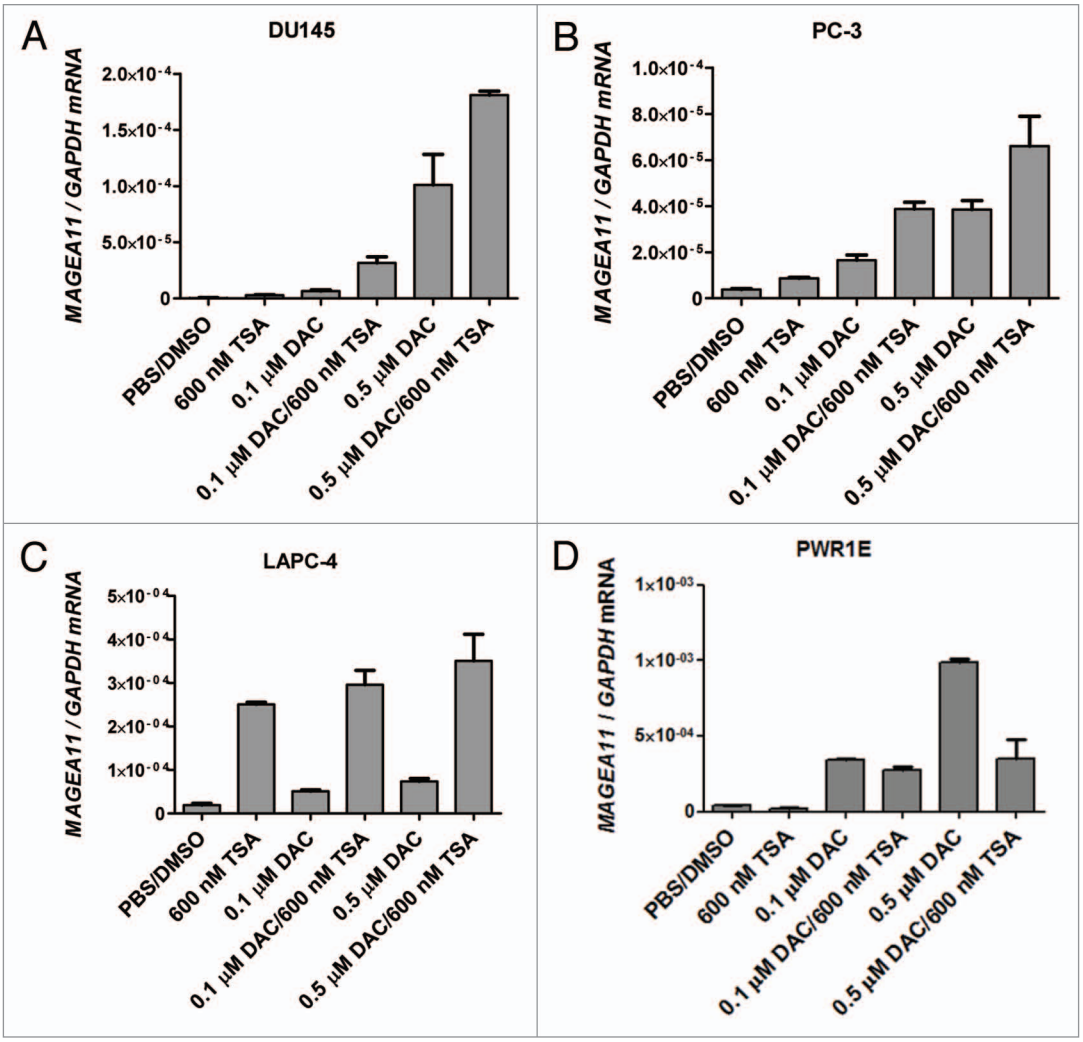

Figure 5. Epigenetic modulatory drugs induce *MAGEA11* expression. *MAGEA11* expression was measured by RT-qPCR following treatment of benign prostate or prostate cancer cell lines with vehicle (PBS/DMSO), Trichostatin A (TSA), and/or decitabine (DAC), as described in "Materials and Methods." (**A**) DU145 cells, (**B**) PC-3 cells, (**C**) LAPC-4 cells, (**D**) PWR-1E cells. We noted that the *MAGEA11/GAPDH* copy number in control LAPC-4 cells appeared substantially lower than observed in other experiments, likely due to repression by DMSO. This effect was also observed in **Figure 7C**.

that Sp1 factors may contribute to *MAGEA11* gene activity. In addition, the data suggested the presence of repressive motifs in the 5' region of *MAGEA11*, based on the lower activity levels of C1 and C2, relative to the C3 construct. It was also notable that DU145 cells showed highest levels of *MAGEA11* promoter activity, while the endogenous *MAGEA11* gene is silenced by DNA methylation in this cell type (**Fig. 6B**; **Fig. 3B**). Thus, DU145 cells may express factors necessary to drive *MAGEA11* expression, but these factors may be restricted at the endogenous gene locus by DNA methylation.

We methylated the C1 through C4 inserts, but not the vector sequences, using HpaII or M.SssI, which methylate 5'-C<u>C</u>GG-3' or 5'-<u>C</u>G-3' sites, respectively, to directly determine the impact of DNA methylation on *MAGEA11* promoter activity. Digestion of the plasmid inserts with HpaII and McrBc restriction enzymes confirmed their expected methylation status (**Fig. 6D**). The results in PC-3 cells are shown in **Figure 6E**. Mock methylated constructs showed a similar pattern of activity as unmethylated constructs, with the C3 construct showing highest activity. Unexpectedly, HpaII, which methylates only 1–2 CpGs in the C1-C4 constructs, strongly repressed *MAGEA11* promoter activity, similar to M.SssI, which methylates all CpG sites in these constructs (**Fig. 6E**). Similar results were obtained in other prostate cell lines (data not shown). The two HpaII sites within the *MAGEA11* promoter region are found within consensus Ets transcription factor binding sites (**Fig. 6C**). Thus, the data suggest that methylation at one or both of these sites impairs *MAGEA11* promoter activity. Consistent with this notion, previous studies have implicated Ets sites in methylation-dependent promoter activity of other *MAGEA* gene family members.[1,17,27,28]

Elevated activity of the C3 construct relative to C4 suggested that Sp1 site binding factors regulate *MAGEA11*. Sp1, the prototype member of the Sp1 family, is expressed widely in benign and malignant tissues, and contributes to oncogenesis.[29] Western blot analysis demonstrated that prostate cell lines express nuclear Sp1 protein (**Fig. 7A**). The Sp1 inhibitor

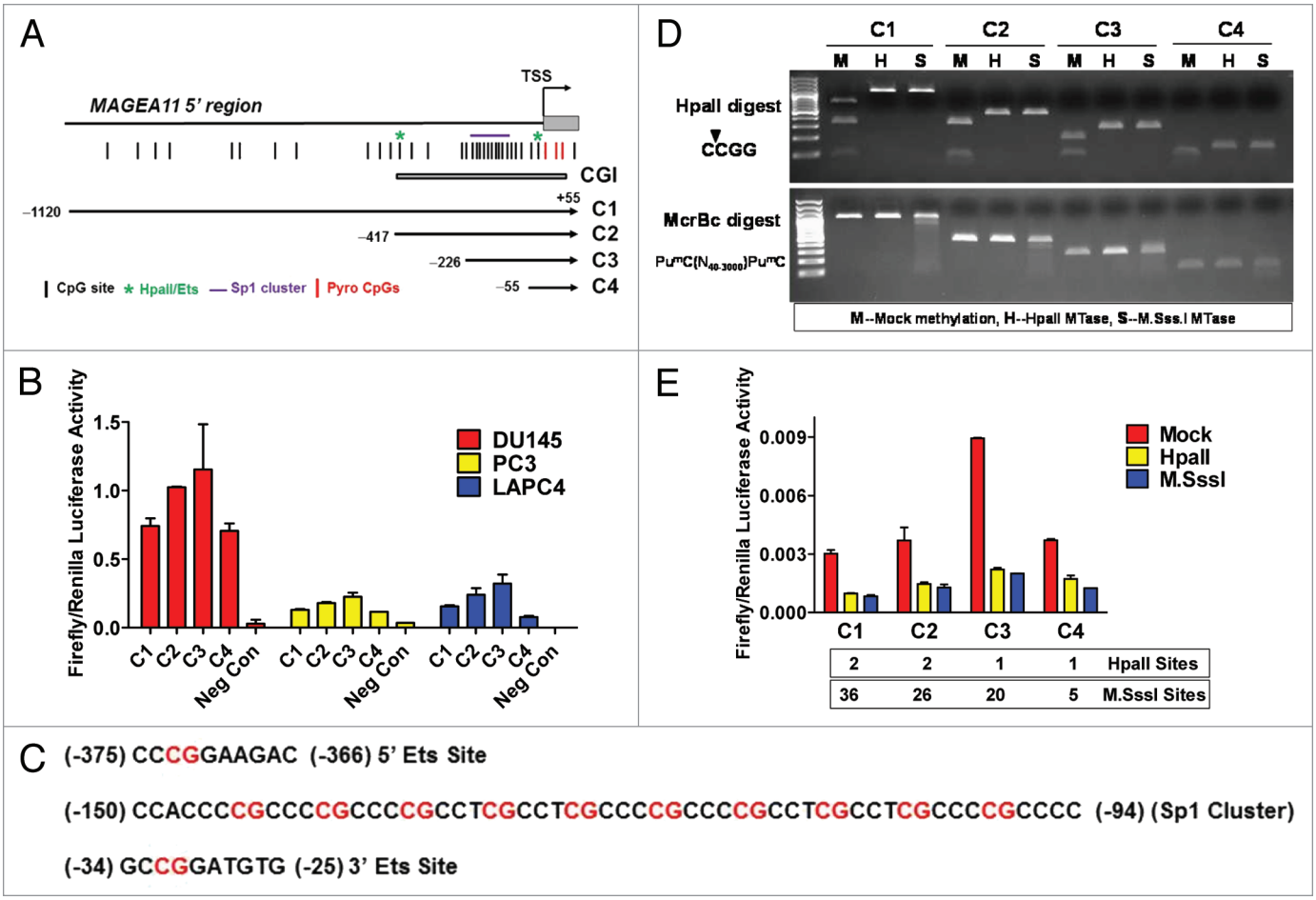

Figure 6. *MAGEA11* promoter activity and repression by DNA methylation. (**A**) Diagram of the *MAGEA11* 5' region and *MAGEA11* promoter luciferase constructs. The *MAGEA11* promoter region, TSS, first part of exon I (gray box), and the CpG island (CGI) are indicated. Four promoter constructs were generated by PCR (C1-C4). The key indicates the location of CpG sites, Ets sites (which correspond to HpaII sites), the Sp1 site cluster, and the three TSS-resident CpG sites examined by bisulfite pyrosequencing. (**B**) C1-C4 constructs were transfected into the indicated prostate cancer cell lines, and promoter activity was measured. Cells treated with the transfection reagent alone served as a negative control. (**C**) Sequence of the two Ets sites and the Sp1 site cluster in the *MAGEA11* promoter. CpG dinucleotides are indicated with red font. The two consensus Ets sites each contain an HpaII recognition sequence (5'-CCGG-3'). The Sp1 cluster contains 10 embedded CpG sites. (**D**) Confirmation of the methylation status of *MAGEA11* promoter construct inserts. Inserts were mock-methylated (M), methylated with HpaII (H), or with M.SssI (S). Methylation status was verified by digestion with HpaII restriction endonuclease (top panel) or McrBc endonuclease (bottom panel). The sequence specificity of each nuclease is shown at left. (**E**) *MAGEA11* promoter repression by methylation. Inserts verified as shown in (**C**) were ligated into the pGL3-basic vector, transfected into PC-3 cells, and promoter activity was measured. The number of HpaII and M.SssI sites in each construct is indicated below the graph.

Mithramycin A (MitA)[30] was used to address whether Sp1 factors are involved in *MAGEA11* regulation. MitA treatment caused a dose-dependent reduction in *MAGEA11* promoter activity and endogenous *MAGEA11* expression in LAPC-4 cells (**Fig. 7B and C**). In addition, decitabine-mediated *MAGEA11* induction in PC-3 cells was inhibited in a dose-dependent manner by MitA treatment (**Fig. 7D**). Furthermore, Sp1 targeting siRNAs reduced *MAGEA11* expression in LAPC-4 cells, proportional to the degree of knockdown (**Fig. 7E and F**). Together, the results demonstrate that Sp1, and potentially related factors, activate *MAGEA11*.

DNA methylation status influences nucleosome occupancy at the *MAGEA11* promoter. DNA methylation and histone modifications can impact gene expression via effects on promoter nucleosome occupancy.[31] Traditional methods to map nucleosome occupancy are based on population averaging, which does not give single molecule information, nor allow integration of endogenous DNA methylation status.[32,33] A newly developed method, MAPit (a.k.a., NOME-seq), overcomes these limitations.[34,35] In MAPit, isolated nuclei are treated with CviP1, an enzyme that methylates nucleosome-free 5'-GC-3' sites.[32] After CviP1 modification, gDNA is recovered and subjected to bisulfite clonal sequencing to simultaneously reveal nucleosome occupancy, as defined by protection from GC methylation, and endogenous DNA methylation, i.e., CG methylation.[36] MAPit allowed us, for the first time, to examine the relationship between DNA methylation and nucleosome occupancy in CG gene regulation, using *MAGEA11* as a model.

To determine whether DNA methylation status influences *MAGEA11* nucleosome occupancy, we utilized the isogenic

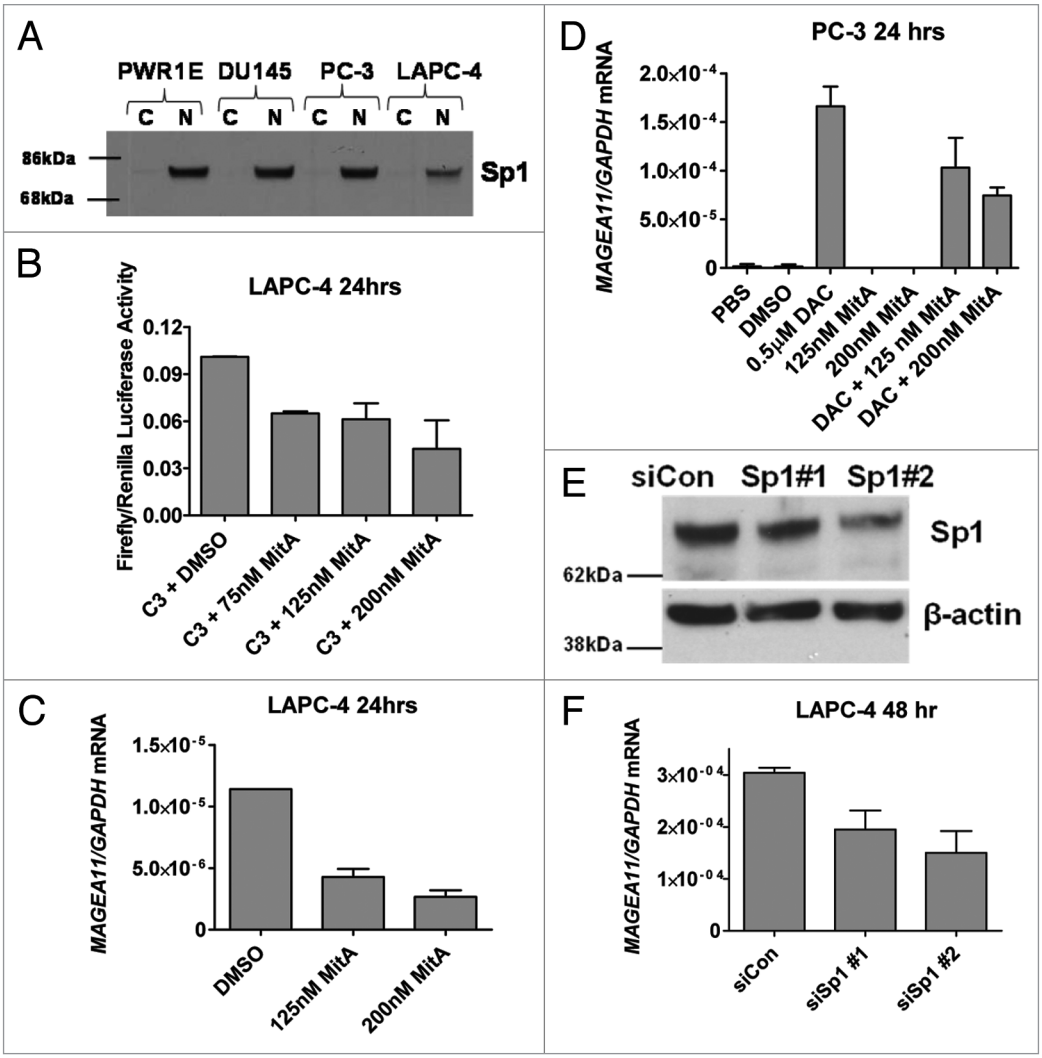

Figure 7. Sp1 contributes to *MAGEA11* promoter activity and gene expression. (**A**) Sp1 protein expression was determined by western blot analysis of the indicated cell lines. C and N refer to cytosolic and nuclear extracts, respectively. (**B**) Mithramycin A (MitA) treatment reduces *MAGEA11* promoter activity. LAPC-4 cells were simultaneously transfected with the C3 construct and treated with DMSO (vehicle) or the indicated concentrations of MitA. Cell extracts were harvested 24 h post-treatment and used for luciferase assay. (**C**) MitA treatment represses *MAGEA11* mRNA expression. LAPC-4 cells were treated with DMSO or MitA for 24 h, and RNA extracts were used to measure *MAGEA11* expression by RT-qPCR. (**D**) MitA treatment suppresses decitabine-mediated *MAGEA11* induction. PC-3 cells were treated with decitabine (DAC) and/or MitA alone or in combination. RNA extracts were harvested five days after initiation of treatment, and were used to measure *MAGEA11* expression by RT-qPCR. (**E**) Sp1 knockdown in LAPC-4 cells. LAPC-4 cells were transfected with two different Sp1 targeting siRNAs, or with a control non-targeting siRNA, once daily for 48 h. 48 h post-treatment, whole cell extracts were prepared and used for western blot analysis. (**F**) Sp1 knockdown reduces *MAGEA11* expression. LAPC-4 cells were treated as described in (**E**), and RNA extracts were prepared 48 h post treatment and used for RT-qPCR analysis of *MAGEA11*.

HCT116/DKO cell model system described earlier.[21] MAPit was conducted on HCT116 wild type and DNMT1/3b knockout (DKO) cells, and the results were analyzed using *MethylViewer*.[37] In agreement with our standard bisulfite clonal sequencing results, *MAGEA11* was hypermethylated at CG sites in HCT116 cells relative to DKO cells (**Fig. 8A and B**). In contrast, GC methylation increased in DKO cells relative to HCT116 wild-type cells, consistent with nucleosome depletion at the *MAGEA11* promoter (**Fig. 8A and B**). Approximately half of the sequenced alleles in DKO cells showed increased CviP1 methylase accessibility. Decitabine-treated HCT116 cells displayed MAPit results similar to DKO cells (data not shown). We noted that the region of the *MAGEA11* promoter with significant variation in GC methylation between HCT116 and DKO cells was localized to the area upstream of the TSS, and spanning approximately 200 bp. This distance is greater than the length of one nucleosome (147 bp), and includes what has been referred to as the -1 nucleosome.[38] In contrast, the areas upstream and downstream showed low GC methylation in both HCT116 and DKO cells, which suggests continued nucleosome occupancy at these locations. Occupancy at the -1 nucleosome position may be critical for *MAGEA11* expression, potentially by impacting RNA Polymerase II (RNAP II) binding.[38] In agreement, ChIP revealed increased RNAP II binding to the *MAGEA11*

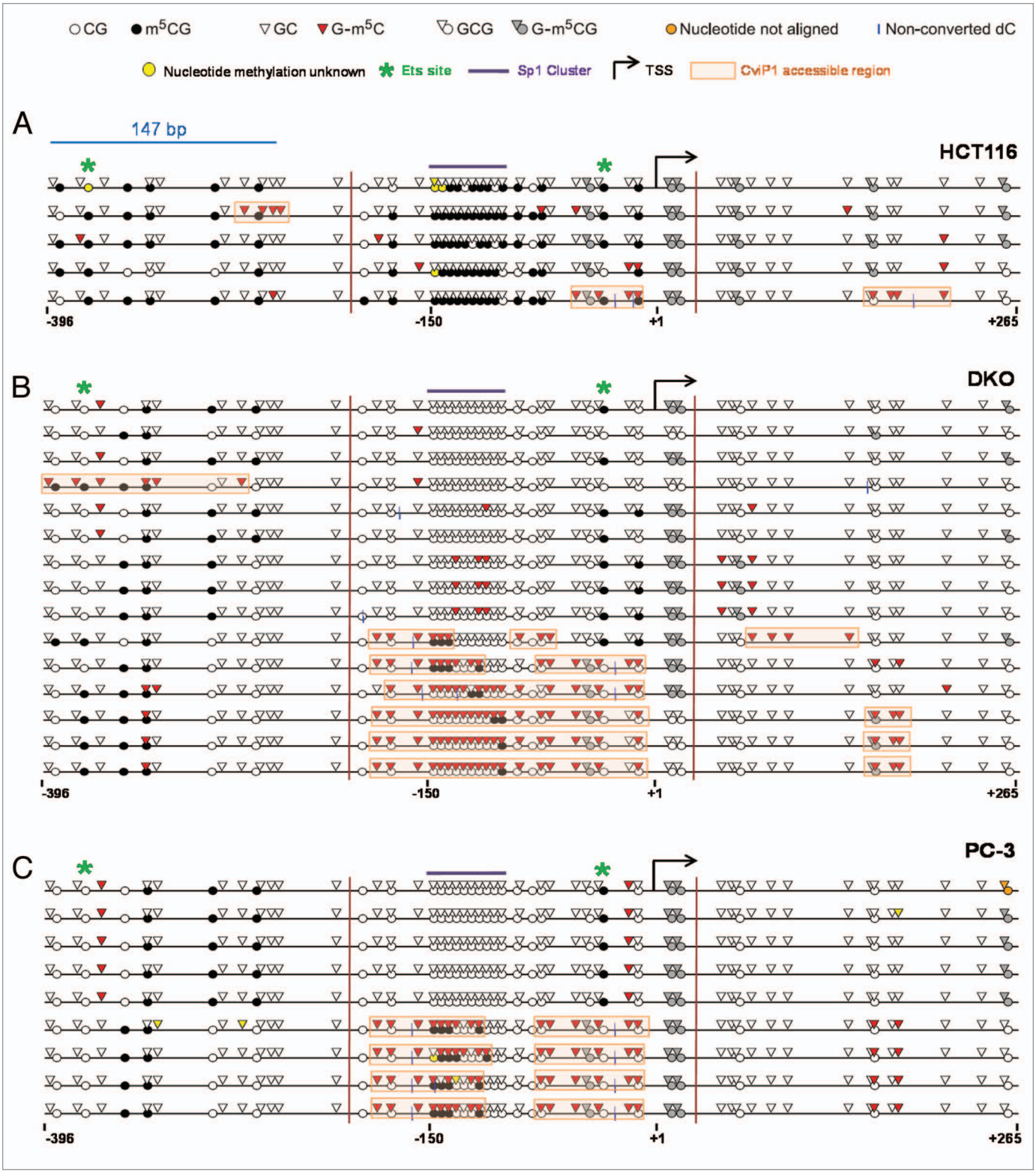

Figure 8. MAPit analysis of *MAGEA11* promoter nucleosome occupancy. MAPit data were analyzed using *MethylViewer*.[37] Each row indicates one individual sequenced allele, and the approximate nucleotide coordinates in relation to the TSS are indicated below each data panel. The key to symbols used is shown at top. The areas highlighted orange indicate CviP1-accessible regions (e.g., nucleosome-free regions) and were defined according to the "3 + 2 rule," i.e., regions of three consecutive G-m^{5}C sites broken by two consecutive GC sites. The vertical magenta lines delineate the termini of the region analyzed by traditional bisulfite clonal sequencing in **Figure S2** (for HCT116 and DKO) and **Figure 3** (for PC-3). (**A**) HCT116 cells. (**B**) DKO cells. (**C**) PC-3 cells.

-1 nucleosome region in DKO cells, relative to HCT116 cells (**Fig. S3B**). In HCT and DKO cells, we additionally noted that the endogenous methylation status of specific CpG sites accurately predicted -1 nucleosome occupancy. Notably, these sites included the 3' HpaII/Ets site mentioned earlier, in the context of luciferase assays (**Fig. 8A and B**).

As shown earlier, the prostate cancer cell line PC-3 displayed low to moderate levels of *MAGEA11* expression along with heterogeneous methylation of the *MAGEA11* 5' CpG island (**Fig. 3A and B**). MAPit analysis of this cell line allowed us to further examine the relationship between *MAGEA11* DNA methylation, gene expression, and nucleosome occupancy. PC-3 cells showed a heterogeneous pattern of nucleosome occupancy, with nucleosome depletion at the -1 nucleosome region in some alleles (**Fig. 8C**). In addition, 3' Ets site methylation was closely associated with nucleosome occupancy in PC-3 cells, as was methylation of two other 5' CpG sites (**Fig. 8C**). Unexpectedly, nucleosome depletion in PC-3 cells correlated with partial methylation at the 5' end of the Sp1 cluster region, while complete hypomethylation of this region correlated with nucleosome occupancy (**Fig. 8C**). This trend was also readily apparent in DKO cells (**Fig. 8B**). Finally, we noted that the region of CviP1 accessibility in the -1 nucleosome region was interrupted by a short stretch of DNA that overlapped the 3' end of the Sp1 cluster region (**Fig. 8C**). This pattern was also observed in some of the sequenced alleles of DKO cells (**Fig. 8B**). The small CviP1-protected region within the larger nucleosome-free -1 region may correspond to a region bound by the transcriptional initiation complex (TIC) and/or a transcription factor. Taken together, our results indicate strong interdependence among DNA methylation, -1 nucleosome occupancy, and *MAGEA11* gene expression.

Discussion

MAGEA11 is a nuclear protein identified in a yeast two-hybrid screen for proteins that bind the human androgen receptor (AR).[39,40] In addition to AR, MAGEA11 is now known to activate human progesterone receptor-B, and its capacity as a steroid receptor activator is in part mediated through interactions with the p300 histone acetyltransferase.[41,42] In addition, MAGEA11 can activate AR signaling by forming a molecular bridge between transcriptionally active AR dimers, and also contributes to prostate cancer cell growth.[4] Most recently, MAGEA11 has been found to promote oncogenesis by targeting the retinoblastoma (RB) pathway.[43] This latter activity may provide the selective pressure for MAGEA11 expression in a variety of human cancers, as reported here. Because of its apparent role in tumorigenesis, MAGEA11 is an important potential target of cancer vaccines and therapeutics. MAGEA11 expression could also serve as a biomarker of cancer prognosis, based on our data showing that *MAGEA11* is expressed in a variety of human cancers, in a manner that correlates both with tumor progression and reduced survival.

MAGEA11 activation in cancer occurs in conjunction with the activation of other CG genes, and in association with DNA hypomethylation at TSS-resident CpG sites. In addition, *MAGEA11* expression and hypomethylation are associated with global DNA hypomethylation, as evidenced both by primary human tumor data from prostate and ovarian cancers, and by data from a genetic DNMT knockout cell system. DNMT and HDAC inhibitors can both activate *MAGEA11* expression, in some cases in a synergistic fashion. Also, we showed that *MAGEA11* promoter activity was repressed directly by DNA methylation and that Sp1, or related factors, contributes to *MAGEA11* promoter activity and endogenous gene expression. For the first time, we have reported the role of nucleosome occupancy in CG antigen gene regulation, using *MAGEA11* as a model. Our MAPit data provide evidence that: (1) DNA methylation specifically regulates nucleosome occupancy at the -1 positioned nucleosome at the *MAGEA11* promoter, (2) methylation of an Ets consensus binding site positioned near the TSS closely correlates with *MAGEA11* -1 nucleosome occupancy, (3) partial methylation at the 5' end of the Sp1 site cluster in the *MAGEA11* promoter CpG island correlates with -1 nucleosome depletion, and (4) a region overlapping the 3' end of the Sp1 site cluster is protected from CviP1 methylation, potentially by binding of the TIC, or by a transcription factor.

Based on the current study, we outline a schematic of events leading to MAGEA11 gene expression in human cancer (**Fig. 9A**). The initiating event driving *MAGEA11* gene expression in cancer is likely to be global DNA hypomethylation. While the underlying cause of global DNA hypomethylation in cancer is yet to be demonstrated,[11] it could reflect alterations of higher-order chromatin structure in the cancer cell nucleus.[44,45] *MAGEA11* TSS hypomethylation is a target of global DNA hypomethylation, and this event provides a chromatin template permissive for gene activation by members of the Ets and Sp1 transcription factor families. Our results also indicate that HDACs contribute to *MAGEA11* gene repression, either as an accessory to DNA methylation or as a primary repressive mechanism in some cancer cells. Full removal of epigenetic repression in certain tumors may allow high level MAGEA11 expression and downstream oncogenic effects (e.g., AR activation in prostate cancer). Conversely, high expression of MAGEA11 may render tumor cells susceptible to immunotherapeutic approaches targeting this antigen.[46] A model for the *MAGEA11* gene configuration in the fully repressed and fully activated state is shown in **Figure 9B**. As indicated, a central aspect of the model is -1 nucleosome occupancy, which is based on the MAPit data. Preliminary analysis of additional cell types, including LAPC-4, also support the importance of -1 nucleosome occupancy in *MAGEA11* regulation (data not shown). The observation that DNA hypomethylation leads to nucleosome depletion at the *MAGEA11 TSS* has increased importance when put in the context of a recent report. Pandiyan et al. showed that only a small subset (<2%) of genes undergoing hypomethylation in DKO cells, or following decitabine treatment, show changes in promoter nucleosome occupancy.[47] The authors proposed that these target genes may be the most important for regulating tumorigenesis in the context of DNA hypomethylation. Experimental validation of *MAGEA11* as one of these targets further suggests an oncogenic role for this

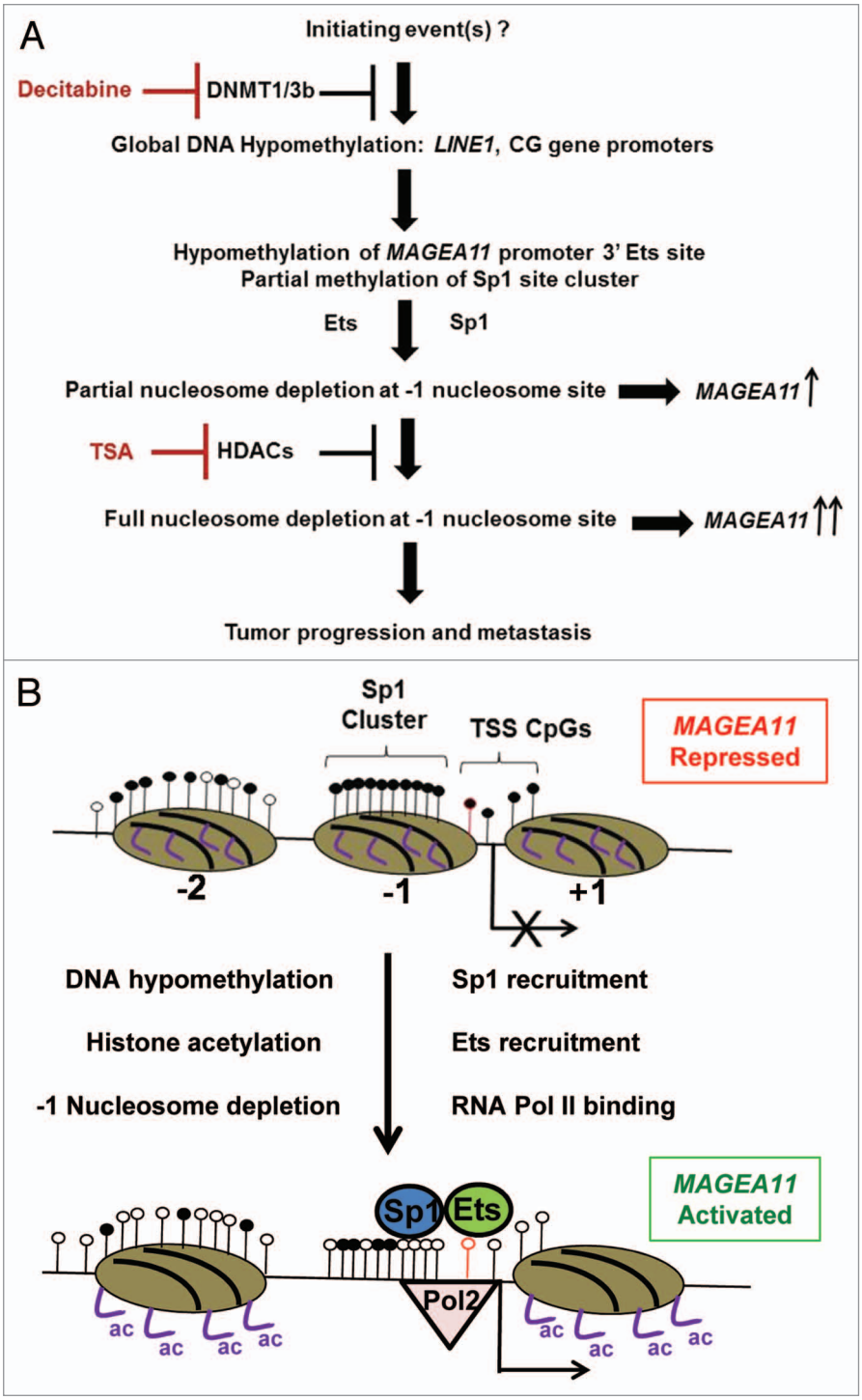

Figure 9. *MAGEA11* gene regulation in human cancer. (**A**) Flowchart of events involved in the activation of *MAGEA11* expression in cancer. (**B**) Schematic of *MAGEA11* promoter configuration in the fully repressed (top) and fully activated states (bottom). Open and filled lollipops indicate unmethylated and methylated CpG sites, respectively. The red outlined lollipop corresponds to the 3' Ets site. Ovals indicate nucleosomes, with numbers below each indicating the nucleosome position relative to the *MAGEA11* TSS. Right bent arrow indicates TSS. Purple lines indicate histone H3 tails. Ac indicates acetylation.

protein. More generally, and also in agreement with the data reported here, a recent report indicated that DNA methylation dictates nucleosome occupancy at numerous genomic loci in human cancer cells.[48]

In addition to revealing a general association between DNA methylation density and nucleosome occupancy at the *MAGEA11* promoter, MAPit also revealed strong correlation between methylation of a specific Ets site and nucleosome occupancy at *MAGEA11*. This finding is particularly striking when considered in the context of our promoter activity data, which demonstrated that methylation at this site alone fully repressed the transcriptional activity of the *MAGEA11* C3 and C4 promoter constructs. In agreement with our observations on *MAGEA11*, other recent work has implicated Ets site hypomethylation in driving the activation of specific genes in cancer.[49] Additional studies are required to define which Ets family member(s) are responsible for *MAGEA11* regulation at this site. While the large size and overlapping target sequences of this protein family will make this task challenging,[50] the question may be amenable to a focused RNAi screening approach.

An additional key finding from MAPit relates to the relationship between methylation of the Sp1 site cluster and nucleosome occupancy. Surprisingly, the *MAGEA11* promoter showed nucleosome depletion only when the Sp1 site cluster was partially (but not fully) methylated. How Sp1 binding is impacted by DNA methylation is controversial, and it appears likely to be based on the specific promoter and cell type.[51-55] Although our preliminary data indicate that Sp1 can directly bind at the *MAGEA11* promoter in prostate cancer cells (data not shown), additional detailed studies are required to determine the epigenetic context in which this binding occurs. Finally, MAPit showed a small CviP1 footprint overlapping the 3' end of the *MAGEA11* Sp1 site cluster, in cells in which the flanking regions were CviP1 accessible (i.e., nucleosome-depleted). This footprint is likely to indicate binding of the TIC, which can occur at Sp1 sites in CpG island promoters that lack a consensus TATA box,[56] as is the case for the *MAGEA11* promoter. Highly similar footprints, potentially related to binding of the TIC, have been observed by others.[57-59] This

footprint could also indicate binding of a Sp1 family member. Resolution of these possibilities is of interest in future studies.

Materials and Methods

In silico gene expression analysis. *Oncomine* (Compendia Bioscience) was used for analysis of *MAGEA11* expression in publically available human microarray data sets. Additional details and references are presented in the Results.

Human cell lines and clinical research tissues. Prostate cell lines and culture conditions were as described.[10] HCT116 wild type and DNMT1/3b single or double knockout (DKO) HCT116 cells and their culture conditions also were as described.[21] Human benign prostatic hyperplasia (BP), androgen-stimulated prostate cancer (AS), castration-recurrent prostate cancer (CR), normal ovary (NO), and epithelial ovarian cancer (EOC) clinical samples were as described.[10,18,19] All EOC tissues contained greater than 90% neoplastic cells. All human tissues were obtained under IRB-approved protocols at the University of North Carolina (prostate) or Roswell Park Cancer Institute (ovarian).

RNA and genomic DNA (gDNA) extractions. RNA was extracted using TRIzol (Invitrogen) according to the manufacturer's instructions. Tissue homogenization was performed as described.[18] RNAs were quantified using Nanodrop (Thermo Scientific) and RNA integrity was assessed using denaturing agarose gel electrophoresis. gDNAs were prepared using the Puregene kit (Qiagen).

Reverse transcriptase quantitative PCR (RT-qPCR). RT-qPCR was used to measure the expression of *MAGEA1*, *NY-ESO-1*, *XAGE-1*, and *GAPDH* as described.[14,19] For *MAGEA11*, the following primers were used: F: 5'-GGAGACTCAGTTCCGCAGAG-3', R: 5'-TGGGACCACT GTAGTTGTGG-3'. Primers were obtained from Integrated DNA Technologies. Briefly, 1 μg of RNA was DNase-treated using the DNA-free kit (Ambion). cDNA was generated using the iScript cDNA synthesis kit (BioRad). Two microliters of 1:5 cDNA sample dilutions were used for qPCR reactions. Standard curves were prepared using gel-purified end-point RT-PCR products amplified from testis RNA. All PCR reactions were performed in triplicate using an Applied Biosystems 7300 System and qPCR MasterMix Plus for SYBR® with ROX master mix (AnaSpec).

Microarray analysis of *MAGEA11* and CG gene expression. Affymetrix HG 1.0ST arrays were used to determine the expression of *MAGEA11* and other CG genes in NO and EOC. Probe generation, array hybridization, and expression analyses were performed by the Next Generation Sequencing and Expression Analysis Core Facility at the University at Buffalo Center for Excellence in Bioinformatics. Samples included three NO and 40 EOC. Correlation between *MAGEA11* expression and other CG genes was determined using the Spearman's test. Full expression data from the microarray analysis will be reported elsewhere.

Determination of the *MAGEA11* transcriptional start site (TSS). RLM-RACE was used to map the *MAGEA11* TSS in LAPC-4 cells, using the First Choice RLM-RACE kit (Ambion, Life Technologies). The following primers were used: Outer PCR: 5'-GTGCTCACCT GGAGTCCAAA-3', Inner PCR: 5'-TTCTTCCTCT TGATGCTGGC-3'. Primers were obtained from Integrated DNA Technologies.

DNA methylation analyses. One microgram gDNA was bisulfite converted using the EZ DNA Methylation Kit (Zymo Research). Bisulfite clonal sequencing of the *MAGEA11* promoter region was performed as described.[10] Bisulfite pyrosequencing was performed to measure methylation of three CpG sites adjacent to the *MAGEA11* TSS. Primers were (forward) 5'-TTTTGTTGTA AATTTAGGGA AGTT-3', (reverse) 5'-biotin-AACCCCACCC TTTATAAAAC TACC-3', and (sequencing) 5'-GGATGTGATT TTTATTGGTT-3'. Primers were obtained from Integrated DNA Technologies. PCR conditions were 10 min × 95 °C, followed by 48 cycles of (95 °C for 30 sec, 57 °C for 30 sec, and 72 °C for one min). Pyrosequencing of the *LINE-1* repetitive element was performed as described.[19] Pyrosequencing was performed using the PSQ HS96 system (Qiagen). Unmethylated and methylated genomic DNA were run as controls. Samples were analyzed in duplicate from separate PCR reactions.

Drug treatments. Various prostate cell lines were treated with 5-aza-2'-deoxycytidine (decitabine, DAC) and/or Trichostatin A (TSA). Decitabine and TSA (Sigma) were solubilized in phosphate buffered saline (PBS) and dimethyl sulfoxide (DMSO), respectively. For decitabine, cells were treated twice, on day 0 and day 2, and harvested on day 4. For TSA, cells were treated on day 0 and harvested on day 1. For combination treatments, cells were treated with decitabine on days 0 and 2, with TSA on day 3, and harvested on day 4. Mithramycin A (MitA) (Sigma) was solubilized in DMSO and added to LAPC-4 cells at 75, 125, or 200 nM. Cell extracts were harvested one day post-treatment, and used for RT-qPCR or luciferase assays as described in Results. PC-3 cells were treated with PBS (vehicle) or decitabine on days 0 and 3, and DMSO (vehicle) or MitA on days 2 and 4, and harvested for RT-qPCR analysis of *MAGEA11* on day 5. As controls for single drug treatments, PC-3 cells were harvested 5 d post-treatment with decitabine or four days post-treatment with MitA.

Chromatin immunoprecipitation (ChIP). ChIP was performed as described.[14] ChIP products were analyzed using end-point PCR and agarose gel electrophoresis, or alternatively using qPCR. qPCR reactions were performed in triplicate using an Applied Biosystems 7300 System and qPCR MasterMix Plus for SYBR® with ROX master mix (AnaSpec). The region flanking the *MAGEA11* TSS was amplified using forward primer 5'-CCTGCTGTAA ATCCAGGGAA-3', and reverse primer 5'-CCCTCTGCCA CTCTCAAGAC-3'. Primers were from Integrated DNA Technologies. ChIP antibodies were H3K9ac (Upstate, Cat#06-599) and RNA Polymerase II (Abcam, Cat #ab5408).

Promoter luciferase assays. Four regions of the *MAGEA11* promoter (C1 through C4) were cloned into pGL3-Basic (Promega) using PCR. Methylation of promoter inserts and religation into pGL3-Basic were as described,[18] except that KpnI and XhoI (Fermentas) were used for digestion. Methylation

reactions utilized M.SssI or HpaII methylases (New England Biolabs). The methylation status of promoter inserts was verified using HpaII or McrBc endonuclease (New England Biolabs) digestions. Transfections utilized Lipofectamine 2000 (Life Technologies). Cell extracts were harvested one day post-transfection. The Dual-Luciferase Reporter Assay System (Promega) was used to determine promoter activity.

Sp1 siRNA knockdown. Pre-designed siRNAs targeting human Sp1 (s13319 [siSp1 #1] and s13320 [siSp1 #2]) were obtained from Ambion (Life Technologies), and siRNA Control Non-Targeting siRNA was obtained from Dharmacon. LAPC-4 cells were transfected with siRNAs using the Lipofectamine 2000 (Life Technologies) reverse transfection method. Cells were transfected with 25 nM siRNA at 0 and 24 h. Cell extracts were collected at 48 h and analyzed using western blot for Sp1, or RT-qPCR for *MAGEA11*.

Western blotting. Proteins were extracted using radioimmunoprecipitation assay (RIPA) buffer, and quantified using the Lowry assay (BioRad). Equal amounts of protein samples per lane were separated using NuPage SDS-PAGE gels (Life Technologies). Alternatively, cytosolic and nuclear protein extracts were prepared using the NE-PER kit (Pierce). Sp1 was detected using Sp1 antibody (Santa Cruz, sc-14027) at 1:200 dilution. β-actin was detected using anti-actin antibody (Santa Cruz, sc-4778) at 1:1000 dilution. Donkey anti-rabbit IgG-HRP secondary antibody (Santa Cruz, sc-2313) was used at 1:5000 dilution. Rabbit anti-mouse IgG-HRP (Santa Cruz, sc-358917) was used at 1:5000 dilution. The Novex ECL HRP Chemiluminescence kit (Life Technologies) was used for protein detection.

Nucleosome occupancy at the *MAGEA11* promoter. Nucleosome occupancy was determined using the Methyltransferase Accessibility Protocol for individual templates (MAPit), also known as Nucleosome Occupancy and Methylome Sequencing (NOME-seq).[33,36,60] Briefly, cell nuclei were isolated and methylated in vitro using 200 units of the 5'-GC-3' methylase CviP1 (New England Biolabs), or mock methylated without enzyme. gDNA was recovered using phenol-chloroform extraction and bisulfite converted using the EZ DNA methylation kit (Zymo). The resulting DNA served as template for PCR of the *MAGEA11* promoter region, using unbiased primers to determine methylation status (forward primer 5'-TAAGAGGAGG ATTTTTTTGA GTGAG-3', reverse primer 5'-AAATAAAACC TCTCCATAAT TTCTCAA-3'), or using a combination of reverse primers selective for amplification of unmethylated (reverse primer 5'-CCTCTACCCA AATCACACCA TA-3') and methylated (reverse primer 5'-CCTCTACCCG AATCACACCA-3') DNA sequences. PCR products were recovered using gel purification (Qiagen), cloned into pTOPO 4.1 (Invitrogen), and subjected to Sanger sequencing. *MethylViewer* was used to analyze MAPit data.[37]

Disclosure of Potential Conflicts of Interest

No potential conflicts of interest were disclosed.

Acknowledgments

We thank Dr Jennifer Black for critical reading of the manuscript, and Leena Forti and Chinaza Egbuta for excellent technical assistance. We thank Dr Michael Kladde and Dr Peter Jones' laboratory for helpful discussions regarding nucleosome occupancy mapping This work was supported by the National Institutes of Health (RO1CA116674 to ARK, P01CA77739 to JLM and EMW), the Ovarian Cancer Research Fund (to ARK and KO), and a State University of New York STEM Doctoral Diversity Fellowship (to CC).

Supplemental Materials

Supplemental materials may be found here:
www.landesbioscience.com/journals/epigenetics/article/25500

References

1. Akers SN, Odunsi K, Karpf AR. Regulation of cancer germline antigen gene expression: implications for cancer immunotherapy. Future Oncol 2010; 6:717-32; PMID:20465387
2. Simpson AJ, Caballero OL, Jungbluth A, Chen YT, Old LJ. Cancer/testis antigens, gametogenesis and cancer. Nat Rev Cancer 2005; 5:615-25; PMID:16034368
3. Meek DW, Marcar L. MAGE-A antigens as targets in tumour therapy. Cancer Lett 2012; 324:126-32; PMID:22634429
4. Minges JT, Su S, Grossman G, Blackwelder AJ, Pop EA, Mohler JL, et al. Melanoma antigen-A11 (MAGE-A11) enhances transcriptional activity by linking androgen receptor dimers. J Biol Chem 2013; 288:1939-52; PMID:23172223
5. Liu W, Cheng S, Asa SL, Ezzat S. The melanoma-associated antigen A3 mediates fibronectin-controlled cancer progression and metastasis. Cancer Res 2008; 68:8104-12; PMID:18829569
6. Cappell KM, Sinnott R, Taus P, Maxfield K, Scarbrough M, Whitehurst AW. Multiple cancer testis antigens function to support tumor cell mitotic fidelity. Mol Cell Biol 2012; 32:4131-40; PMID:22869527
7. Whitehurst AW, Xie Y, Purinton SC, Cappell KM, Swanik JT, Larson B, et al. Tumor antigen acrosin binding protein normalizes mitotic spindle function to promote cancer cell proliferation. Cancer Res 2010; 70:7652-61; PMID:20876808
8. Whitehurst AW, Bodemann BO, Cardenas J, Ferguson D, Girard L, Peyton M, et al. Synthetic lethal screen identification of chemosensitizer loci in cancer cells. Nature 2007; 446:815-9; PMID:17429401
9. Renaud S, Loukinov D, Alberti L, Vostrov A, Kwon YW, Bosman FT, et al. BORIS/CTCFL-mediated transcriptional regulation of the hTERT telomerase gene in testicular and ovarian tumor cells. Nucleic Acids Res 2011; 39:862-73; PMID:20876690
10. Karpf AR, Bai S, James SR, Mohler JL, Wilson EM. Increased expression of androgen receptor coregulator MAGE-11 in prostate cancer by DNA hypomethylation and cyclic AMP. Mol Cancer Res 2009; 7:523-35; PMID:19372581
11. Ehrlich M. DNA hypomethylation in cancer cells. Epigenomics 2009; 1:239-59; PMID:20495664
12. Karpf AR. Epigenetic alterations in oncogenesis. Preface. Adv Exp Med Biol 2013; 754:v-vii; PMID:23189391
13. Cannuyer J, Loriot A, Parvizi GK, De Smet C. Epigenetic hierarchy within the MAGEA1 cancer-germline gene: promoter DNA methylation dictates local histone modifications. PLoS One 2013; 8:e58743; PMID:23472218
14. James SR, Link PA, Karpf AR. Epigenetic regulation of X-linked cancer/germline antigen genes by DNMT1 and DNMT3b. Oncogene 2006; 25:6975-85; PMID:16715135
15. Link PA, Gangisetty O, James SR, Woloszynska-Read A, Tachibana M, Shinkai Y, et al. Distinct roles for histone methyltransferases G9a and GLP in cancer germ-line antigen gene regulation in human cancer cells and murine embryonic stem cells. Mol Cancer Res 2009; 7:851-62; PMID:19531572
16. Wischnewski F, Pantel K, Schwarzenbach H. Promoter demethylation and histone acetylation mediate gene expression of MAGE-A1, -A2, -A3, and -A12 in human cancer cells. Mol Cancer Res 2006; 4:339-49; PMID:16687489
17. Karpf AR, Lasek AW, Ririe TO, Hanks AN, Grossman D, Jones DA. Limited gene activation in tumor and normal epithelial cells treated with the DNA methyltransferase inhibitor 5-aza-2'-deoxycytidine. Mol Pharmacol 2004; 65:18-27; PMID:14722233
18. Woloszynska-Read A, James SR, Link PA, Yu J, Odunsi K, Karpf AR. DNA methylation-dependent regulation of BORIS/CTCFL expression in ovarian cancer. Cancer Immun 2007; 7:21; PMID:18095639
19. Woloszynska-Read A, Mhawech-Fauceglia P, Yu J, Odunsi K, Karpf AR. Intertumor and intratumor NY-ESO-1 expression heterogeneity is associated with promoter-specific and global DNA methylation status in ovarian cancer. Clin Cancer Res 2008; 14:3283-90; PMID:18519754

20. Woloszynska-Read A, Zhang W, Yu J, Link PA, Mhawech-Fauceglia P, Collamat G, et al. Coordinated cancer germline antigen promoter and global DNA hypomethylation in ovarian cancer: association with the BORIS/CTCF expression ratio and advanced stage. Clin Cancer Res 2011; 17:2170-80; PMID:21296871
21. Rhee I, Bachman KE, Park BH, Jair KW, Yen RW, Schuebel KE, et al. DNMT1 and DNMT3b cooperate to silence genes in human cancer cells. Nature 2002; 416:552-6; PMID:11932749
22. Song L, James SR, Kazim L, Karpf AR. Specific method for the determination of genomic DNA methylation by liquid chromatography-electrospray ionization tandem mass spectrometry. Anal Chem 2005; 77:504-10; PMID:15649046
23. Rao M, Chinnasamy N, Hong JA, Zhang Y, Zhang M, Xi S, et al. Inhibition of histone lysine methylation enhances cancer-testis antigen expression in lung cancer cells: implications for adoptive immunotherapy of cancer. Cancer Res 2011; 71:4192-204; PMID:21546573
24. Yoshida M, Kijima M, Akita M, Beppu T. Potent and specific inhibition of mammalian histone deacetylase both in vivo and in vitro by trichostatin A. J Biol Chem 1990; 265:17174-9; PMID:2211619
25. Egger G, Liang G, Aparicio A, Jones PA. Epigenetics in human disease and prospects for epigenetic therapy. Nature 2004; 429:457-63; PMID:15164071
26. Campbell MJ, Turner BM. Altered histone modifications in cancer. Adv Exp Med Biol 2013; 754:81-107; PMID:22956497
27. De Plaen E, Naerhuyzen B, De Smet C, Szikora JP, Boon T. Alternative promoters of gene MAGE4a. Genomics 1997; 40:305-13; PMID:9119398
28. De Smet C, De Backer O, Faraoni I, Lurquin C, Brasseur F, Boon T. The activation of human gene MAGE-1 in tumor cells is correlated with genome-wide demethylation. Proc Natl Acad Sci U S A 1996; 93:7149-53; PMID:8692960
29. Li L, Davie JR. The role of Sp1 and Sp3 in normal and cancer cell biology. Ann Anat 2010; 192:275-83; PMID:20810260
30. Blume SW, Snyder RC, Ray R, Thomas S, Koller CA, Miller DM. Mithramycin inhibits SP1 binding and selectively inhibits transcriptional activity of the dihydrofolate reductase gene in vitro and in vivo. J Clin Invest 1991; 88:1613-21; PMID:1834700
31. Henikoff S. Nucleosomes at active promoters: unforgettable loss. Cancer Cell 2007; 12:407-9; PMID:17996642
32. Pondugula S, Kladde MP. Single-molecule analysis of chromatin: changing the view of genomes one molecule at a time. J Cell Biochem 2008; 105:330-7; PMID:18615586
33. Miranda TB, Kelly TK, Bouazoune K, Jones PA. Methylation-sensitive single-molecule analysis of chromatin structure. Current protocols in molecular biology/edited by Frederick M Ausubel [et al.] 2010; Chapter 21:Unit 21 17 1-6.
34. You JS, Kelly TK, De Carvalho DD, Taberlay PC, Liang G, Jones PA. OCT4 establishes and maintains nucleosome-depleted regions that provide additional layers of epigenetic regulation of its target genes. Proc Natl Acad Sci U S A 2011; 108:14497-502; PMID:21844352
35. Jessen WJ, Dhasarathy A, Hoose SA, Carvin CD, Risinger AL, Kladde MP. Mapping chromatin structure in vivo using DNA methyltransferases. Methods 2004; 33:68-80; PMID:15039089
36. Pardo CE, Darst RP, Nabilsi NH, Delmas AL, Kladde MP. Simultaneous single-molecule mapping of protein-DNA interactions and DNA methylation by MAPit. Current protocols in molecular biology/edited by Frederick M Ausubel [et al.] 2011; Chapter 21:Unit 21 2.
37. Pardo CE, Carr IM, Hoffman CJ, Darst RP, Markham AF, Bonthron DT, et al. MethylViewer: computational analysis and editing for bisulfite sequencing and methyltransferase accessibility protocol for individual templates (MAPit) projects. Nucleic Acids Res 2011; 39:e5; PMID:20959287
38. Bai L, Morozov AV. Gene regulation by nucleosome positioning. Trends Genet 2010; 26:476-83; PMID:20832136
39. Bai S, He B, Wilson EM. Melanoma antigen gene protein MAGE-11 regulates androgen receptor function by modulating the interdomain interaction. Mol Cell Biol 2005; 25:1238-57; PMID:15684378
40. Jurk M, Kremmer E, Schwarz U, Förster R, Winnacker EL. MAGE-11 protein is highly conserved in higher organisms and located predominantly in the nucleus. Int J Cancer 1998; 75:762-6; PMID:9495246
41. Su S, Blackwelder AJ, Grossman G, Minges JT, Yuan L, Young SL, et al. Primate-specific melanoma antigen-A11 regulates isoform-specific human progesterone receptor-B transactivation. J Biol Chem 2012; 287:34809-24; PMID:22891251
42. Askew EB, Bai S, Blackwelder AJ, Wilson EM. Transcriptional synergy between melanoma antigen gene protein-A11 (MAGE-11) and p300 in androgen receptor signaling. J Biol Chem 2010; 285:21824-36; PMID:20448036
43. Su S, Minges JT, Grossman G, Blackwelder AJ, Mohler JL, Wilson EM. Proto-oncogene activity of Melanoma antigen-A11 (MAGE-A11) regulates Retinoblastoma-related p107 and E2F1. J Biol Chem 2013; In press.
44. Berman BP, Weisenberger DJ, Aman JF, Hinoue T, Ramjan Z, Liu Y, et al. Regions of focal DNA hypermethylation and long-range hypomethylation in colorectal cancer coincide with nuclear lamina-associated domains. Nat Genet 2012; 44:40-6; PMID:22120008
45. Reddy KL, Feinberg AP. Higher order chromatin organization in cancer. Semin Cancer Biol 2013; 23:109-15; PMID:23266653
46. Karpf AR. A potential role for epigenetic modulatory drugs in the enhancement of cancer/germ-line antigen vaccine efficacy. Epigenetics 2006; 1:116-20; PMID:17786175
47. Pandiyan K, You JS, Yang X, Dai C, Zhou XJ, Baylin SB, et al. Functional DNA demethylation is accompanied by chromatin accessibility. Nucleic Acids Res 2013; 41:3973-85; PMID:23408854
48. Portela A, Liz J, Nogales V, Setién F, Villanueva A, Esteller M. DNA methylation determines nucleosome occupancy in the 5'-CpG islands of tumor suppressor genes. Oncogene 2013; PMID:23686312
49. Bi FF, Li D, Yang Q. Hypomethylation of ETS Transcription Factor Binding Sites and Upregulation of PARP1 Expression in Endometrial Cancer. Biomed Res Int 2013; 2013:946268; PMID:23762867
50. Hollenhorst PC, McIntosh LP, Graves BJ. Genomic and biochemical insights into the specificity of ETS transcription factors. Annu Rev Biochem 2011; 80:437-71; PMID:21548782
51. Harrington MA, Jones PA, Imagawa M, Karin M. Cytosine methylation does not affect binding of transcription factor Sp1. Proc Natl Acad Sci U S A 1988; 85:2066-70; PMID:3281160
52. Höller M, Westin G, Jiricny J, Schaffner W. Sp1 transcription factor binds DNA and activates transcription even when the binding site is CpG methylated. Genes Dev 1988; 2:1127-35; PMID:3056778
53. Clark SJ, Harrison J, Molloy PL. Sp1 binding is inhibited by (m)Cp(m)CpG methylation. Gene 1997; 195:67-71; PMID:9300822
54. Mancini DN, Singh SM, Archer TK, Rodenhiser DI. Site-specific DNA methylation in the neurofibromatosis (NF1) promoter interferes with binding of CREB and SP1 transcription factors. Oncogene 1999; 18:4108-19; PMID:10435592
55. Mulero-Navarro S, Carvajal-Gonzalez JM, Herranz M, Ballestar E, Fraga MF, Ropero S, et al. The dioxin receptor is silenced by promoter hypermethylation in human acute lymphoblastic leukemia through inhibition of Sp1 binding. Carcinogenesis 2006; 27:1099-104; PMID:16410262
56. Butler JE, Kadonaga JT. The RNA polymerase II core promoter: a key component in the regulation of gene expression. Genes Dev 2002; 16:2583-92; PMID:12381658
57. Darst RP, Pardo CE, Pondugula S, Gangaraju VK, Nabilsi NH, Bartholomew B, et al. Simultaneous single-molecule detection of endogenous C-5 DNA methylation and chromatin accessibility using MAPit. Methods Mol Biol 2012; 833:125-41; PMID:22183592
58. Lin JC, Jeong S, Liang G, Takai D, Fatemi M, Tsai YC, et al. Role of nucleosomal occupancy in the epigenetic silencing of the MLH1 CpG island. Cancer Cell 2007; 12:432-44; PMID:17996647
59. Delmas AL, Riggs BM, Pardo CE, Dyer LM, Darst RP, Izumchenko EG, et al. WIF1 is a frequent target for epigenetic silencing in squamous cell carcinoma of the cervix. Carcinogenesis 2011; 32:1625-33; PMID:21873353
60. Kilgore JA, Hoose SA, Gustafson TL, Porter W, Kladde MP. Single-molecule and population probing of chromatin structure using DNA methyltransferases. Methods 2007; 41:320-32; PMID:17309843
61. Chandran UR, Ma C, Dhir R, Bisceglia M, Lyons-Weiler M, Liang W, et al. Gene expression profiles of prostate cancer reveal involvement of multiple molecular pathways in the metastatic process. BMC Cancer 2007; 7:64; PMID:17430594
62. Nanni S, Priolo C, Grasselli A, D'Eletto M, Merola R, Moretti F, et al. Epithelial-restricted gene profile of primary cultures from human prostate tumors: a molecular approach to predict clinical behavior of prostate cancer. Mol Cancer Res 2006; 4:79-92; PMID:16513839
63. Cancer Genome Atlas Research Network. Integrated genomic analyses of ovarian carcinoma. Nature 2011; 474:609-15; PMID:21720365
64. Hu N, Clifford RJ, Yang HH, Wang C, Goldstein AM, Ding T, et al. Genome wide analysis of DNA copy number neutral loss of heterozygosity (CNNLOH) and its relation to gene expression in esophageal squamous cell carcinoma. BMC Genomics 2010; 11:576; PMID:20955586
65. Aoyagi K, Minashi K, Igaki H, Tachimori Y, Nishimura T, Hokamura N, et al. Artificially induced epithelial-mesenchymal transition in surgical subjects: its implications in clinical and basic cancer research. PLoS One 2011; 6:e18196; PMID:21533028
66. Cutcliffe C, Kersey D, Huang CC, Zeng Y, Walterhouse D, Perlman EJ; Renal Tumor Committee of the Children's Oncology Group. Clear cell sarcoma of the kidney: up-regulation of neural markers with activation of the sonic hedgehog and Akt pathways. Clin Cancer Res 2005; 11:7986-94; PMID:16299227
67. Zhao H, Ljungberg B, Grankvist K, Rasmuson T, Tibshirani R, Brooks JD. Gene expression profiling predicts survival in conventional renal cell carcinoma. PLoS Med 2006; 3:e13; PMID:16318415